Theoretical investigation on the $N+SF_2 \rightarrow NS^+$ reaction involving resonance-enhanced multiphoton ionization process

Ya-Jun Liu
Department of Chemistry, Graduate School, Chinese Academy of Sciences, P.O. Box 3908, Beijing 100039, People's Republic of China, and Research Institute of Computational Quantum Chemistry, Hebei Normal University, Shijiazhuang, 050091, People's Republic of China

Ming-Bao Huang[a)]
Department of Chemistry, Graduate School, Chinese Academy of Sciences, P.O. Box 3908, Beijing 100039, People's Republic of China

Xiao-Guo Zhou, Quan-Xin Li, and Shu-Qin Yu
Open Laboratory of Bond-selective Chemistry, Department of Chemical Physics, University of Science and Technology of China, Hefei, Anhui, 230026, People's Republic of China

(Received 18 March 2002; accepted 23 July 2002)

NS^+ was detected from ionization of the final product of the $N(^2D)+SF_2$ reaction by laser multiphoton ionization. NS is not the spectral carrier of our REMPI (resonance-enhanced multiphoton ionization) spectrum. For understanding the experimental facts and to obtain a complete description of the whole process, quantum-chemical calculations were performed. The density functional theory/Becke's three-parameter hybrid-function calculations indicate that NSF is the product of the most favorable channel of the $N+SF_2$ reaction. The complete active space self-consistent field (CASSCF) potential energy curve calculations predict that $1\,^1A''$ is a predissociative state of NSF with the NS radical and F atom as the dissociation products. The CASSCF vibrational frequencies calculated at the $1\,^1A''$ minimum are in line with the excitation spectrum. The CASPT2 adiabatic excitation energy value of 3.32 eV for the $1\,^1A''$ state is close to the energy value (3.44 eV) of one photon. On the basis of theoretical calculations, it is concluded that NS^+ detected in the experiments is produced by one-photon dissociation and ionization of the $1\,^1A''$ excited state of NSF, which is the product of the most favorable channel of the $N+SF_2$ reaction. © *2002 American Institute of Physics.* [DOI: 10.1063/1.1506917]

I. INTRODUCTION

There is considerable interest in SF_2 because of its great importance in semiconductor manufacturing, and it is believed that SF_2 plays a significant role in plasma etching by SF_6 and O_2.[1–4] For more than 10 years, spectroscopic studies on the electronic excited states of SF_2 have been carried out by several groups.[5–11] After extensive successful spectroscopic studies, investigation of the reactivity of SF_2 has become an interesting topic.

In this work, we carried out an experimental study of the SF_2 reaction with the nitrogen atom. The $N(^2D)+SF_2$ reaction system was produced by dc electric discharge, and the product was detected, as NS^+, by time-of-flight mass spectrometer using the REMPI (resonance-enhanced multiphoton ionization) spectroscopy method. We obtained a vibrationally resolved REMPI excitation spectrum by measuring the m/z 46 (NS^+) ion signal as a function of laser wavelength, the vibrational separation of which is about 300 cm^{-1} (one-photon energy), and the spectrum is shown in Fig. 1. However, our REMPI excitation spectra is completely different from the reported $(2+1)$ REMPI excitation spectrum $F\,^2\Delta(3d\delta) \leftarrow X$ of NS radical between 320 and 360 nm.[12] Furthermore, the rotationally resolved spectrum at peak 6 of Fig. 1 is far from the typical rotational spectrum of NS. It is clear that NS is not the spectral carrier of our REMPI excitation spectrum. It is natural to assume that the NS^+ signals come from NSF (or NSF_2) through REMPID (resonance-enhanced multiphoton ionization dissociation) or REMPDI (resonance-enhanced multiphoton dissociation ionization) processes. However, the information from the experiments is not sufficient to obtain a complete description of the whole process. To understand the experimental facts and give a complete description for the whole process, we have carried out theoretical study by performing quantum-chemical calculations. The DFT (density functional theory[13,14]) B3LYP (Becke's three-parameter hybrid function[15] with the nonlocal correlation of Lee–Yang–Parr[16]) method was used in the calculations for the ground-state reaction of the $N+SF_2$ system, and NSF is found to be the product of the most favorable channel. The CASPT2 and CASSCF methods were used in the calculations of vertical excitation energies (T_v) and dissociation processes of electronic excited states of NSF. In the present paper we give a preliminary description for our experiments on the basis of our theoretical calculations.

II. CALCULATION DETAILS

We first briefly describe the apparatus and methods used in the experiments. A pulsed dc discharge system was used to

a)Electronic mail: mbhuang@yeah.net

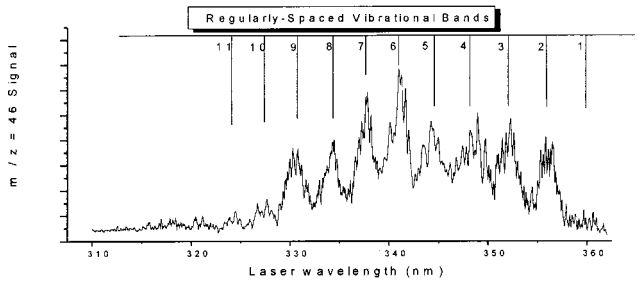

FIG. 1. REMPI excitation spectrum of m/z 46 ion signals between 320 and 360 nm.

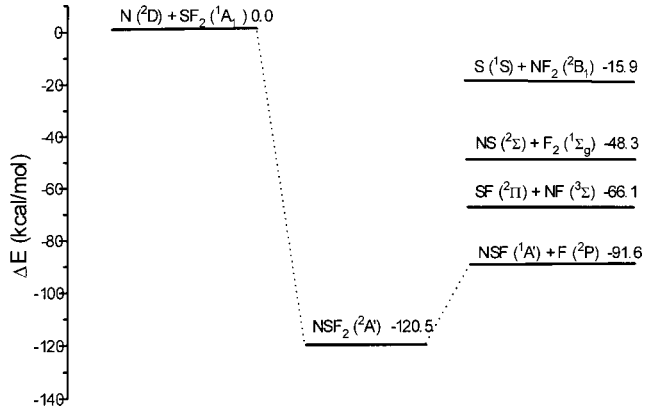

FIG. 2. The reaction channels of the $N+SF_2$ reaction. Values are the B3LYP/6-311+G(d) relative energies (in kcal/mol) of the products and the NSF_2 intermediate.

generate the reactants. The light source used was a dye laser (Lumonics: HT500) pumped with the Nd:YAG laser (Spectral Physics: GCR-170). The dye laser output was frequency doubled with a doubler (Lumonics: HT1000). The ions generated by the REMPI processes were detected by a time-of-flight mass spectrometer and analyzed with a computer data acquisition system.

The DFT B3LYP calculations for the $N(^2D)+SF_2$ reaction were carried out using a 6-311+G(d) basis set.[17] All possible channels of the reaction should be considered. The reaction path calculations for a reaction channel should include geometry optimization calculations to locate stationary points along the path, frequency analysis calculations for characterizing the stationary points as intermediates or transition states, and IRC calculations starting at the transition states. The B3LYP calculations were carried out using the GAUSSIAN 94W programs.[18]

The CASPT2 method was used in the vertical excitation energy (T_v) calculations for the three lowest-lying $^1A'$ and the three lowest-lying $^1A''$ states of NSF (the potential spectral carrier) at its experimental ground-state geometry [R (N–S)=1.446 Å, R (S–F)=1.646 Å, and $\angle$NSF=116.9°].[19] For each symmetry (A' or A'') one more root was calculated for technical reasons, and the state-average technique was used. With a CASSCF wave function constituting the reference function, the CASPT2 method computes the first-order wave function and the second-order energy in full-CI space without any further approximation.[20,21] In the definition of zeroth-order Hamiltonian, the full Fock matrix was used (PT2F). The CASSCF method was used in the calculations of the potential energy curves, along the dimension associated with the S–F bond distance, of the four lowest-lying singlet electronic states of NSF. The calculations of a potential energy curve of a specific electronic state include a set of CASSCF (partial) geometry optimization calculations for that state at fixed values of the S–F bond distance. We also carried out the frequency calculations for the stationary points on the potential energy curves using the CASSCF method.

In the CASSCF (and CASPT2) calculations, 14 electrons were active. Labeling the orbitals within the C_s point group in the order of a' and a'', an active space named (84) was used. The atomic natural orbital (ANO) basis sets,[22–24] N(10s6p3d)/[3s2p1d], F(10s6p3d)/[3s2p1d], and S(13s10p4d)/[4s3p2d], were used in CASSCF potential energy curve calculations. In the CASPT2 T_v calculations, we supplemented this set of basis with an 1s1p1d Rydberg basis (obtained by following the procedure implimented in MOLCAS 5.0 quantum-chemistry software[25] and placed at the charge centroid of the NSF^+ cation). The CASSCF and CASPT2 calculations were performed using MOLCAS 5.0[25] quantum-chemistry software.

III. CALCULATION RESULTS AND DISCUSSION

The theoretical study for understanding our experiments consists of three steps. Different calculation methods were used for different steps, and the targets (molecular systems or electronic states) calculated in each step were determined based on the analysis of the calculation results of the former step.

A. B3LYP calculations for the $N(^2D)+SF_2$ reaction

The products of all the possible channels of the $N(^2D)+SF_2$ reaction are shown in Fig. 2, and there are four: NSF+F, SF+NF, NS+F_2, and S+NF_2. All the products and the reactants [$N(^2D)+SF_2$] are assumed to be in the lowest-lying doublet potential surface of the reaction system.

The B3LYP/6-311+G(d) relative energies of the four product groups relative to the reactants are also given in Fig. 2. The product group, NSF+F, is predicted to be 91.6 kcal/mol more stable than the reactants and to have the lowest energy among the four product groups. The other three product groups, SF+NF, NS+F_2, and S+NF_2, are predicted to be 25.5, 43.3, and 75.7 kcal/mol higher in energy than the NSF+F product group, respectively.

The B3LYP/6-311+G(d) reaction path calculations were carried out for the $N+SF_2 \rightarrow NSF+F$ reaction channel, and we found only one stationary point (the NSF_2 adduct) along the path, which is characterized as an intermediate by the B3LYP/6-311+G(d) frequency analysis calculations. Since there is no transition state along the reaction path, the IRC calculations are not needed. It is concluded that the $N+SF_2 \rightarrow NSF+F$ channel is the most favorable channel of the $N+SF_2$ reaction. NSF is the potential spectral carrier of our REMPI excitation spectrum and would be the source of the NS radical.

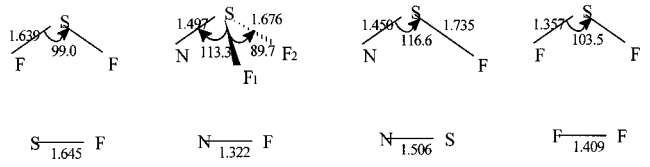

FIG. 3. The B3LYP/6-311+G(d) optimized geometries of the reactants, products, and the NSF_2 intermediate in the $N+SF_2$ reaction. Bond lengths are in Å and angles in deg.

The reaction path calculations for the other three channels were not performed. Those calculations should be considered if there were transition state(s) along the reaction path of the $N+SF_2 \rightarrow NSF+F$ channel. The paths for the other three channels might be complicated, and they might or might not pass through NSF_2.

The B3LYP/6-311+G(d) optimized geometries of the reactants, products of all the four channels, and the NSF_2 intermediate are given in Fig. 3. We comment on the B3LYP/6-311+G(d) geometry of NSF below.

B. CASPT2 vertical excitation energy calculations for NSF

The electronic excited states of the potential spectral carrier, NSF, were examined, and the CAS methods were used for excited state calculations. We used the CASPT2 method for the vertical excitation energy calculations since the CASPT2 calculations predict more accurate excitation energies than the CASSCF calculations.

The CASPT2 T_v calculations were performed at the experimental ground-state geometry of NSF [R(N–S) =1.446 Å, R(S–F)=1.646 Å, and ∠NSF=116.9°].[19] Here, we mention that we also have theoretical geometries for NSF in the ground state ($X\,^1A'$): the B3LYP/6-311+G(d) geometry shown in Fig. 3 and the CASSCF geometry shown in Fig. 4. The two theoretical geometries for the NSF ground state are similar. The S–F bond lengths in the two theoretical geometries are about 0.1 Å longer than that in the experimental geometry, though the theoretical values for the N–S bond length and the NSF angle are close to the respective experimental values.[19] Eventually we used the experimental ground-state geometry.

The purpose of our CASPT2 T_v calculations was to find excited states of NSF lying below 6.68 eV, which is the sum value of the energies of two photons used in the experiments (more photons and higher-lying excited states were not considered). In Table I the CASPT2 vertical excitation energies for the three lowest-lying $^1A''$ states and the three lowest-lying $^1A'$ states ($1\,^1A'=X\,^1A'$) of NSF are listed, together with the CASSCF expectation value of x^2 (the x coordinate is perpendicular to the NSF molecular plane) and the weights (ω) of the reference configurations in the first-order wave functions in the CASPT2 calculations.

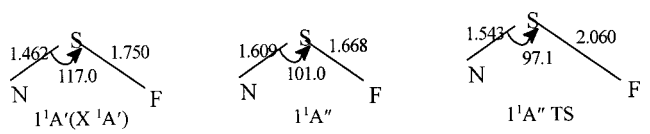

FIG. 4. The equilibrium geometries of $X\,^1A'$ and $1\,^1A''$ states predicted by the CASSCF optimization calculations, together with the CASSCF geometry of the transition state along the $1\,^1A''$ potential energy curve. Bond lengths are in Å and angles in deg.

TABLE I. CASPT2 vertical excitation energies (T_v) of the lowest-lying singlet electronic states of NSF, calculated at the experimental ground-state geometry [R (N–S)=1.446 A, R (S–F)=1.646 A, and ∠NSF=116.9°] reported in Ref. 19.

	CASPT2			
State	ω[a]	$\langle x^2\rangle$[b]	n_{states}[c]	T_v
$X\,^1A'$	0.920	62.1	1–4	0.00
$1\,^1A''$	0.912	60.3	1–4	3.60
$2\,^1A''$	0.911	59.6	1–4	5.39
$2\,^1A'$	0.906	61.8	1–4	6.12
$3\,^1A''$	0.901	59.6	1–4	7.57
$3\,^1A'$	0.898	60.0	1–4	7.63

[a]The weights of the CASSCF reference configurations in the first-order wave functions.
[b]CASSCF expectation value (in a.u.^{2}) of x^2, where x is the coordinate perpendicular to the molecular plane.
[c]States included in the state-average CASSCF calculations.

The CASPT2 T_v calculations predict the following energy ordering (the T_v ordering) for the six electronic states of NSF: $X\,1\,^1A'$, $1\,^1A''$, $2\,^1A''$, $2\,^1A'$, $3\,^1A''$, and $3\,^1A'$ (see Table I). The CASPT2 T_v values for the $3\,^1A''$ and $3\,^1A'$ states are larger than 6.88 eV. The CASPT2 T_v values for the $1\,^1A''$, $2\,^1A''$, and $2\,^1A'$ excited states of NSF are smaller than 6.88 eV (see Table I), and these states would be investigated further (see below).

The expectation value of x^2 can be used to identify the character of an excited state: valence or Rydberg. The expectation values for the five excited states are between 59.6–61.8 a.u.^{2}, which are close to the value (62.1 a.u.^{2}) for the ground state. Therefore, all five excited states can be identified as valence excited states.

C. CASSCF potential energy curve calculations for excited states of NSF

The main purpose of the CASSCF potential energy curve calculations for the $X\,^1A'$, $1\,^1A''$, $2\,^1A''$, and $2\,^1A'$ states of NSF was to get information about the general features of these curves. The calculated curves are those along the dimension associated with the S–F bond distance. The potential energy curve calculations for each of the four states involve a set of CASSCF (partial) geometry optimizations: at each of the fixed values of the S–F bond distance [R(S–F)], the other two geometric parameters were optimized.

The CASSCF potential energy curves, along the dimension associated with the S–F bond distance, of the $X\,^1A'$, $1\,^1A''$, $2\,^1A''$, and $2\,^1A'$ states of NSF are shown in Fig. 5. As shown in Fig. 5, the $X\,^1A'$ state is a bound state as expected and the $2\,^1A''$ and $2\,^1A'$ states are repulsive. The feature of the $1\,^1A''$ curve will be discussed in detail below. The dissociation products of the four states are the same: the NS radical plus the F atom, which are both neutral and in their respective ground states. It is noted that the $2\,^1A''$ state lies above the $2\,^1A'$ state at the R(S–F) values between 1.5

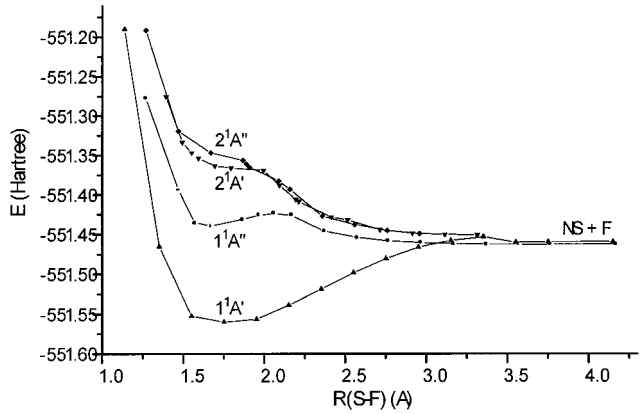

FIG. 5. The CASSCF potential energy curves, along the dimension associated with the S–F bond distance [R(S–F)], of the $X\,^1A'$, $1\,^1A''$, $2\,^1A'$, and $2\,^1A''$ states of NSF.

Å and 1.8 Å, and the two states have close energy values at other R(S–F) values. This fact implies that the CASSCF T_v ordering for the six electronic states might be slightly different from the CASPT2 T_v ordering of Table I. The $2\,^1A''$ and $2\,^1A'$ states may interchange in the T_v orderings.

There are two stationary points along the $1\,^1A''$ curve. One is located at the R(S–F) value of 1.668 Å. Frequency analysis calculations indicate that this stationary point is a minimum-energy point with the following three vibration frequencies: $v_3(\mathrm{N–S–F}) = 319.0\ \mathrm{cm}^{-1}$, $v_1(\mathrm{N–S}) = 901.4\ \mathrm{cm}^{-1}$, and $v_2(\mathrm{S–F}) = 662.9\ \mathrm{cm}^{-1}$. The other stationary point along the $1\,^1A''$ curve is located at the R(S–F) value of 2.060 Å, which is a transition state (the unique imaginary frequency being 526.7 cm^{-1}). The general feature of the $1\,^1A''$ curve indicates that $1\,^1A''$ is a predissociative state.

As shown in Fig. 1, a progression of $\sim 300\ \mathrm{cm}^{-1}$ (single-photon energy) was measured. This vibrational interval suggests a low frequency bending vibration of a molecule consisting of heavy atoms. Additionally, the broadened vibration peaks in the REMPI excitation spectrum imply dissociation from the parent molecule to fragments. Assuming NSF in the $1\,^1A''$ state as the parent molecule, the present band spacing ($\sim 300\ \mathrm{cm}^{-1}$) is in reasonable agreement with the calculated bending vibration frequency [$v_3(\mathrm{N–S–F}) = 319.0\ \mathrm{cm}^{-1}$]. Moreover, the other vibration frequencies [$v_1(\mathrm{N–S}) = 901.4\ \mathrm{cm}^{-1}$ and $v_2(\mathrm{S–F}) = 662.9\ \mathrm{cm}^{-1}$] are close to three and two times the bending vibrational frequency, respectively. Therefore, the observed vibration progression in Fig. 1 possibly involves resonance excitation of three vibronic modes and their mixing modes.

We also performed CASPT2 (single point) calculation in some regions of the four potential energy curves, and it is confirmed that only the $1\,^1A''$ state is a predissociative state. The potential energy curve calculations clearly indicate that the $1\,^1A''$ excited state of NSF is a predissociative state with the NS radical and F atom as the dissociation products. The barrier energy was calculated as the energy difference between the two stationary points along the $1\,^1A''$ curve, and it is predicated to be 0.43 and 0.28 eV at the CASSCF and CASPT2 (//CASSCF) levels, respectively. The CASPT2 adiabatic excitation energy (T_0) of $1\,^1A''$ excited state was calculated using the experimental ground-state geometry[19] and the CASSCF equilibrium geometry of the $1\,^1A''$ state (the CASSCF optimized geometry for the minimum-energy point); it is predicted to be 3.32 eV, which is close to the energy value (3.44 eV) of one photon used in the experiments.

In Fig. 4 are given the CASSCF optimized equilibrium geometries of $X\,^1A'$ and $1\,^1A''$ states, together with the CASSCF optimized geometry for the $1\,^1A''$ transition state (saddle point). We have already mentioned the B3LYP equilibrium geometry of $X\,^1A'$ state in subsection A, which is very similar to its CASSCF optimized geometry.

Based on the above calculation results, it is concluded that the REMPI excitation spectrum is attributed to an one-photon resonant transition from the $X\,^1A'$ ground state to $1\,^1A''$ excited state of NSF, and the NS^+ signals were yielded from the $1\,^1A''$ excited state of NSF through dissociation and ionization processes.

IV. CONCLUSION

The $N + SF_2$ reaction induced by dc discharge was experimentally studied by using the REMPI technique. The NS^+(m/z=46) signals were detected, while the NS radical is found not to be the spectral carrier of our REMPI excitation spectrum. To understand the experiments and give a complete description of the whole process, quantum-chemical calculations were performed. The B3LYP calculations indicate that the $N + SF_2 \rightarrow NSF + F$ channel is the most favorable channel, and therefore NSF is the potential spectral carrier of our REMPI excitation spectrum and would be the source of NS^+. The CASPT2 vertical excitation energy (T_v) calculations for NSF indicate that there are three excited states, $1\,^1A''$, $2\,^1A''$, and $2\,^1A'$, having their T_v values smaller than the sum value (6.88 eV) of the energies of two photons used in the experiments. The CASSCF calculations for the potential energy curves, along the dimension associated with the S–F bond distance, of the $X\,^1A'$, $1\,^1A''$, $2\,^1A''$, and $2\,^1A'$ states of NSF were performed. The potential energy curve calculations indicate that $1\,^1A''$ is a predissociative state, and its dissociation products are the NS radical and F atom in their respective ground states. The CASSCF vibrational frequencies calculated at the $1\,^1A''$ minimum are in line with the excitation spectrum. The CASPT2 adiabatic excitation energy value of 3.32 eV for the $1\,^1A''$ state is close to the energy value (3.44 eV) of one photon. On the basis of theoretical calculations, it is concluded that NS^+ detected in the experiments was produced by one-photon dissociation and ionization of the $1\,^1A''$ excited state of NSF, which is the product of the most favorable channel of the $N + SF_2$ reaction and the spectral carrier of our REMPI excitation spectrum.

ACKNOWLEDGMENTS

This work was supported by the National Natural Science Foundation Committee of China (20173056, 20173197, 29892162, and 29873046), the Department of Science and

Technology of China (No. G199907530), and the Research Fund for the Doctoral Program of Higher Education (1999035828).

[1] R. D'Agostino and D. L. Flamm, J. Appl. Phys. **52**, 162 (1981).
[2] F. J. Janssenn and J. G. Kema, Sci. Tech. Rep. **2**, 9 (1984).
[3] G. D. Griffin, C. E. Easterly, I. Sauers, H. W. Ellis, and L. G. Christophorou, Tox. Environ. Chem. **9**, 139 (1984).
[4] K. R. Ryan and I. C. Plumb, Plasma Chem. Plasma Process. **8**, 263 (1988).
[5] R. J. Glinski, Chem. Phys. Lett. **129**, 342 (1986).
[6] R. J. Glinski and C. D. Taylor, Chem. Phys. Lett. **155**, 511 (1989).
[7] R. J. Glinski, C. D. Taylor, and F. W. Kutzler, J. Phys. Chem. **94**, 6196 (1990).
[8] R. D. Johnson III and J. W. Hudgens, J. Phys. Chem. **94**, 3273 (1990).
[9] Q. X. Li, J. N. Shu, Q. Zhang, S. Q. Yu, L. M. Zhang, C. X. Chen, and X. X. Ma, J. Phys. Chem. A **102**, 7233 (1998).
[10] Q. X. Li, Q. Zhang, J. N. Shu, S. Q. Yu, Q. H. Song, C. X. Chen, and X. X. Ma, Chem. Phys. Lett. **305**, 79 (1999).
[11] Y.-J. Liu, M.-B. Huang, X. Zhou, and S. Yu, Chem. Phys. Lett. **345**, 505 (2001).
[12] M. Barnes, J. Baker, J. M. Dyke, and R. Richter, Chem. Phys. **185**, 433 (1991).
[13] P. Hohenberg and W. Kohn, Phys. Rev. **136**, B864 (1964).
[14] W. Kohn and L. Sham, Phys. Rev. **140**, A1133 (1965).
[15] A. D. Becke, J. Chem. Phys. **98**, 5648 (1993).
[16] C. Lee, W. Yang, and R. G. Parr, Phys. Rev. B **37**, 785 (1988).
[17] P. v. R. Schleyer and J. A. Pople, *Ab Initio Molecular Orbital Theory* (Wiley, New York, 1986).
[18] M. J. Frisch, G. W. Trucks, H. B. Schlegel *et al.*, GAUSSIAN 94W, Revision E.1, Gaussian, Inc., Pittsburgh, PA, 1995.
[19] D. O. Cowan, R. Gleiter, O. Glemser, E. Heilbronner, and J. Schaublin, Helv. Chim. Acta **54**, 1559 (1971).
[20] K. Andersson, P.-A. Malmqvist, B. O. Roos, A. J. Sadlej, and K. Wolinski, J. Phys. Chem. **94**, 5483 (1990).
[21] K. Andersson, P.-A. Malmqvist, and B. O. Roos, J. Chem. Phys. **96**, 1218 (1992).
[22] J. Almlof and P. R. Taylor, J. Chem. Phys. **86**, 4070 (1987).
[23] P.-O. Widmark, P.-A. Malmqvist, and B. O. Roos, Theor. Chim. Acta **77**, 291 (1990).
[24] P.-O. Widmark, B.-J. Persson, and B. O. Roos, Theor. Chim. Acta **79**, 419 (1991).
[25] K. Andersson, M. P. Fulscher, R. Lindh, P.-A. Malmqvist, J. Olsen, A. J. Sadlej, and P.-O. Widmark, MOLCAS version 5.0, University of Lund, Sweden, 2000.